LASER MICROMACHINING OF SILICON: A NEW TECHNIQUE FOR FABRICATING HIGH QUALITY TERAHERTZ WAVEGUIDE COMPONENTS[1]

C. K. Walker, G. Narayanan, H. Knoepfle, J. Capara, J. Glenn, A. Hungerford
Steward Observatory, University of Arizona, Tucson, AZ 85721

and

T. M. Bloomstein, S. T. Palmacci, M. B. Stern, and J. E. Curtin
Lincoln Laboratory, Massachusetts Institute of Technology, Lexington, MA 02173

ABSTRACT

One of the main obstacles encountered in designing low noise, high efficiency, heterodyne receivers and local oscillator sources at submillimeter wavelengths is the quality and cost of waveguide structures. At wavelengths shorter than 400 micrometers, rectangular waveguide structures, feedhorns, and backshorts become extremely difficult to fabricate using standard machining techniques. We have used a new laser milling technique to fabricate high quality, THz waveguide components and feedhorns. Once metallized, the structures have the properties of standard waveguide components. Unlike waveguide components made using silicon wet-etching techniques, laser-etched components can have almost any cross section, from rectangular to circular. Under computer control, the entire waveguide structure (including the corrugated feedhorn!) of a submillimeter-wave mixer or multiplier can be fabricated to micrometer tolerances in a few hours. Laser etching permits the direct scaling of successful waveguide multiplier and mixer designs to THz frequencies. Since the entire process is computer controlled, the cost of fabricating submillimeter waveguide components is significantly reduced. With this new laser etching process, the construction of high

---

performance waveguide array receivers at THz frequencies becomes tractable. In this paper we describe the laser etching technique and discuss test results from a micromachined 2 THz feedhorn.

1 Motivation

The vast majority of radio receivers, transmitters, and components that operate at millimeter and submillimeter wavelengths utilize waveguide structures in some form. This is because waveguide is a well characterized, low-loss, transmission medium which can be readily fashioned into a variety of high-quality circuit and quasi-optical components. The long history of development of waveguide components provides a broad base of knowledge from which to synthesize and evaluate new designs. In addition, new computer aided design tools (*e.g.* Hewlett Packard's High Frequency Structure Simulator) provide a straightforward way of optimizing even complicated waveguide structures. Unfortunately, at frequencies above 1 THz, waveguide dimensions become so small (less than 0.23 by 0.116 mm) that fabrication utilizing conventional machining and electroforming techniques becomes extremely difficult, expensive, and/or impossible. Indeed, for situations where even modest sized heterodyne array receivers are being considered, the practical frequency limit to utilizing conventional machined waveguide structures is much lower ($\sim$ 500 GHz). This situation is unfortunate, since, due to their lower loss and tuning flexibility, waveguide mixers have been found to (in general) outperform quasi-optical mixers both electrically and optically at frequencies where both have been constructed. Clearly, a new way of machining small waveguide structures is needed in order to reap the benefits of waveguide at THz freqencies.

In the past, silicon wet etching techniques have been employed as an alternative to conventional machining [1, 2]. The main disadvantage of the wet etching technique is that one is forced to follow the $< 100 >$ or $< 110 >$ crystal plane in the silicon. This severely limits the types of structures that can be produced. The process is well suited to making wide-angle pyramidal horns or straight sections of single height waveguide. However, it cannot readily be used to make waveguide structures in which the height of the waveguide is stepped down (*e.g.* in an impedance transformer) or tapered (either rectangular or circular). These structures are needed to make efficient feedhorns.

In this paper we introduce a new laser micromachining technique for fabricating high quality, low-cost waveguide structures for frequencies up to ~ 10 THz. With this process, waveguide components of varying height and width can be machined to ~ 1 μm accuracy. As a test of the viability of the laser micromachining technology, we conducted beam pattern measurements on a 2 THz corrugated feedhorn made using this process.

2 Waveguide Fabrication

2.1 Laser Induced Microchemical Etching of Silicon

Laser processing offers several advantages for machining parts in the micro-domain. Compared to conventional machining, smaller feature sizes with greater mechanical tolerances can typically be achieved due to the high focusability of laser light and ability to deliver intense sources of energy with high precision. Since laser machining is a non-contact process, there is no mechanically-induced material damage, tool-wear, or machine vibration from cutting forces. This can lead to finer finishes, improved accuracy, and less process overhead. A number of different materials ranging from metals and polymers to composites and ceramics have been successfully machined using lasers, traditionally using ablative techniques.

For the waveguide application, we employ a laser-induced microreaction initially developed for trimming and trench etching of silicon in semiconductor microfabrication [3,4,5]. As explained below, there are several important advantages to using chemical action for the controlled removal of material. The basic process is shown schematically in Figure 1. An argon-ion laser is used to locally heat a portion of the silicon substrate in a chlorine ambient. At the onset of melting, volatile silicon chlorides are formed. Due to the highly non-linear activation energy of the process, the reaction is confined almost exclusively to the molten zone. Also, silicon is bound into volatile products unlike ablative techniques which due to their explosive nature, can lead to particulate formation. These are often very difficult to remove due to significant attractive forces in the micro-domain. Chemical activation also reduces the energy requirement for removal minimizing the potential for cracking. Using a crystalline material such as silicon also has the benefit that unetched portions of the molten zone regrow epitaxially to crystalline quality. This allows controlled thin shavings to be removed plane
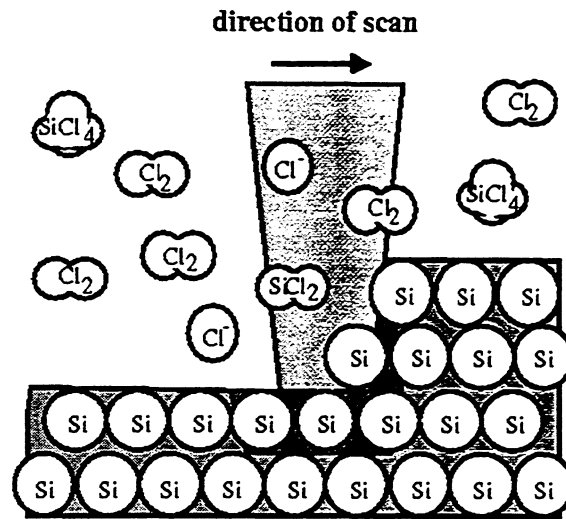
Figure 1: Schematic representation of laser direct write etching of silicon in a chlorine ambient. Using high NA optics, the reaction zone can be confined to the necessary micrometer resolutions demanded for microelectronics processing.

by plane with no change in etch rate. In this manner, structures can be built up by limiting the etch depth at each scan plane [6,7].

In practice, this etch depth can be maintained to approximately one micrometer shavings using low-inertia galvanometers to rapidly deflect the beam. The basic set-up of the optical scanning system and vapor cell used are similar to those of previously developed laser-direct write systems [8]. As shown schematically in Figure 2, the output of a 15-Watt argon ion laser is expanded to a 16 mm beam using an 8× telescope. The beam is deflected using a commercial X-Y scanner [9] through an achromatic lens which serves as the focusing element. The focused beam is introduced through a quartz cover-glass into a stainless-steel vapor cell containing the sample. The vapor cell has ports for gas inlet and outlet, pressure head, and thermocouple. The wafer surface is typically biased to approximately 100° C using an IR-illumination source incident on the substrate from the backside. Filtered, 99.9% pure research grade chlorine is slowly flowed over the wafer surface at 20 SCCM to limit the build-up of products. A cold trap is also placed before the vacuum pump to protect it
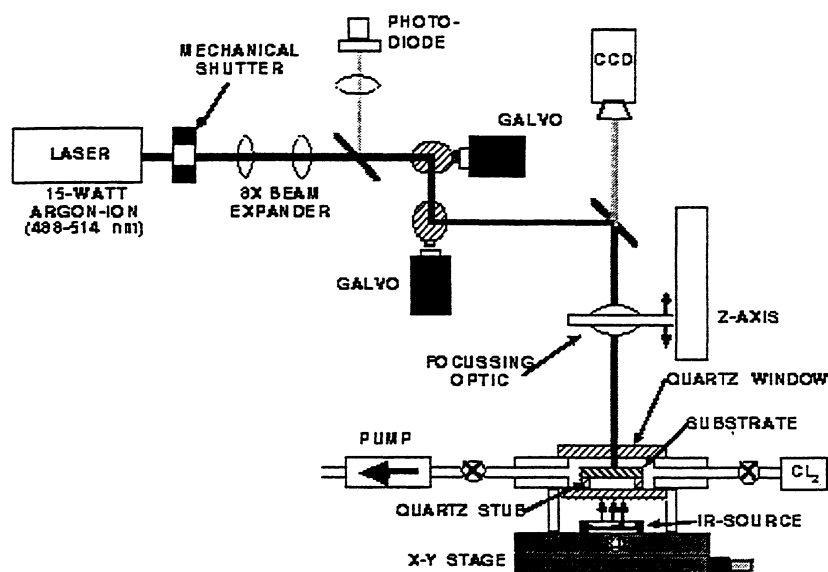
Figure 2: Schematic diagram of galvanometer based scanning apparatus. A higher power objective (not shown) can be slid in place of the focusing optic to allow more detailed analysis of the surface. For etching high aspect ratio structures, a circular polarizer is placed in the beam path to improve edge uniformity due to the selective reflectivity of the S and P polarization components along the side-walls.

from the corrosive gas. The reaction is observed through the focusing optic with a charge coupled device (CCD) camera. A high power 50× objective is also mounted on a linear translation stage containing the focusing element allowing details on the surface to be more closely examined in-situ. The scanning system is driven directly from computer generated patterns which can be constructed using a commercial solid-modeling software package or via software using a toolbox of simple shapes.

A detailed description of the process physics can be found in [10]. Below, we summarize the results. The volumetric removal rate (Vol Rate) is found experimentally to scale according

to:

$$\text{Vol Rate} = 10^4 \mu\text{m}^2/\text{s}(\text{T}_\text{A}/300\text{K})^{0.8}\omega_\text{m}$$

where T_A is the temperature of the ambient gas and ω_m is the diameter of the molten zone. The proportionality constant is determined by the complicated transport and reaction dynamics, particularly from gas phase chemical reactions which alter the dynamics through compositional changes and heats of reaction. The temperature scaling is due to the improved diffusive transport of species to and from the chemically active area in the gas-phase localized above the molten zone. The gas ambient temperature (equal to the bias temperature of the substrate) can be continually increased to approximately 700 K. At higher temperatures, significant background etching of the substrate occurs. Additional laser energy can also initiate a self-sustained reaction leading to highly damaged and coarse looking surfaces. The removal rate is also found to scale directly with the radius of the molten zone. This linear scaling of removal rate with reaction zone is characteristic of systems with three dimensional transport such as in the combustion of fuel droplets. The melt zone diameter is dependent on the laser power, optical coupling, and thermal properties of silicon. In practice, the melt zone can be varied from 1 to 25 μm using a 15 Watt argon-ion laser running multi-mode. This leads to removal rates ranging from approximately 10^4 $\mu\text{m}^3/\text{s}$ (0.036 mm^3/hr) to 5×10^5 $\mu\text{m}^3/\text{s}$ (1.8 mm^3/hr). By virtue of the scaling law, smaller, higher frequency waveguide components can be fabricated in *even less* time since volumetric removal rates scale linearly with melt zone diameter, or resolution, while the total volume of the device scales cubically with length scale. For instance, a similar 1.62 THz waveguide at 4-μm resolution can be etched in one-fourth the time of an 810 GHz version etched at 8-μm resolution.

As an example of a laser micromachined part, a proof-of-concept demonstration was made of a portion of an 810 GHz and 2 THz circular to rectangular mode matching waveguide. In the initial prototyping of the 810 GHz waveguide structure, an approximately 8 μm diameter laser-induced reaction zone (6-μm laser beam spot size) is swept across the surface at 5 cm/s removing 1 μm shavings per plane at a rate of $10^5 \mu\text{m}^3/\text{s}$. Higher scanning velocities can be used to increase depth resolution. Improved lateral resolutions, if necessary, are possible over critical dimensions through power modulation of the laser beam. Figure 3 shows a portion of the waveguide structure etched in 1 hour (a duplicate mating piece must be fabricated). A larger portion of the feedhorn is shown in Figure 4. For the 2 THz
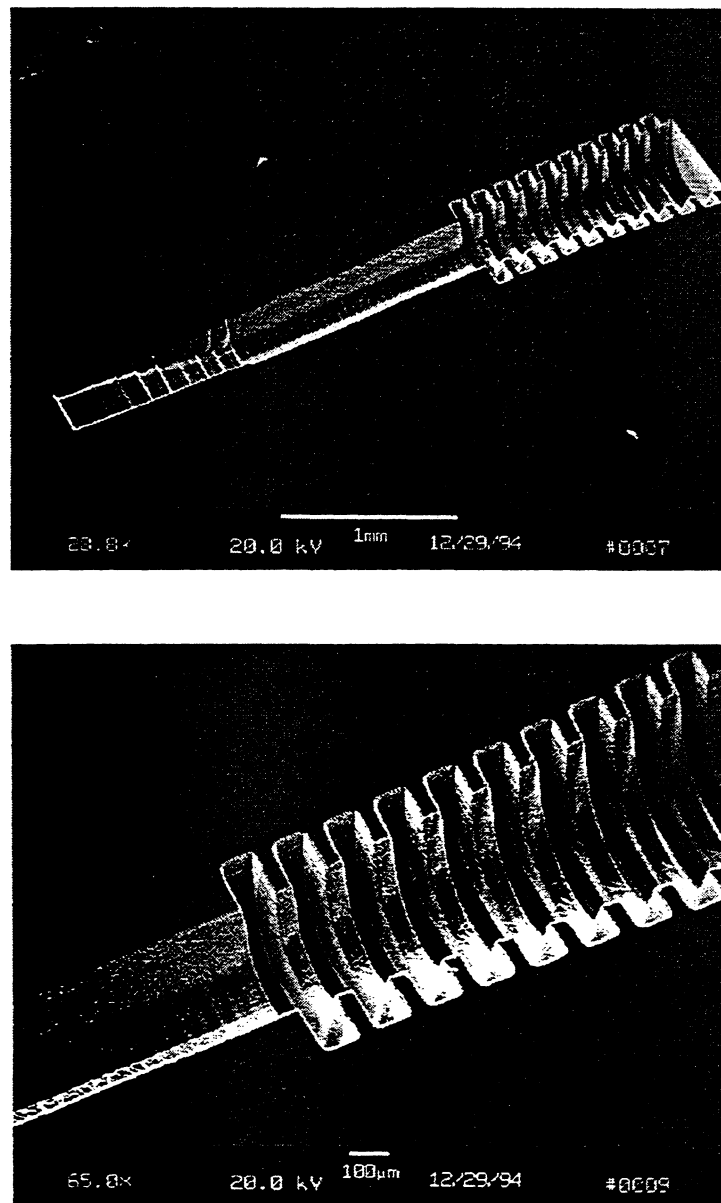
Figure 3: (a) Scanning Electron Micrograph (SEM) of portion of an 810 GHz feedhorn structure. The structure was etched using 4.3 Watts of laser power focused into a 6 μm spot in 200 Torr of chlorine gas. The laser beam was scanned at 5 cm/s and incrementally moved 2 micrometers between line scans. Under these conditions, nominally 1 μm shavings are removed per pass of the laser over the surface. The total etch time is one hour, not including the overhead time for pattern generation and stage motion. (b) SEM close-up of ridges.
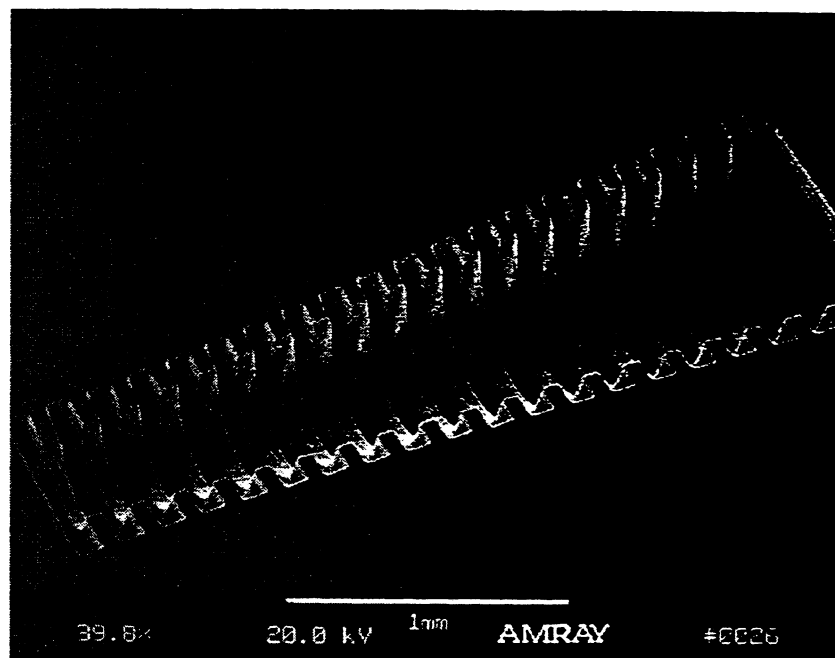
Figure 4: SEM of the first twenty-ridges in the feedhorn portion of the 810 GHz structure. The same processing conditions described in Figure 3 were used. This extended portion of the feedhorn required two hours to fabricate, not including the overhead time for pattern generation and stage motion.

device, an approximately 4 μm (3-μm laser beam spot size) diameter laser-induced reaction zone is swept across the surface at 4 cm/s removing 0.65 μm shavings per plane at a rate of $5 \times 10^4 \mu\text{m}^3/\text{s}$. Figure 5 show scanning electron micrographs of the structures.

Waveguide surface roughness values measured with atomic force microscopy are typically on the order of 200 nm RMS. This surface quality is already sufficient to provide low-loss waveguide performance to $\geq$ 10 THz. The RMS surface roughness can be reduced even further, to under 25 nm, using standard polishing etches based on $HF-HNO_3-HC_2H_3O_2$ solutions.
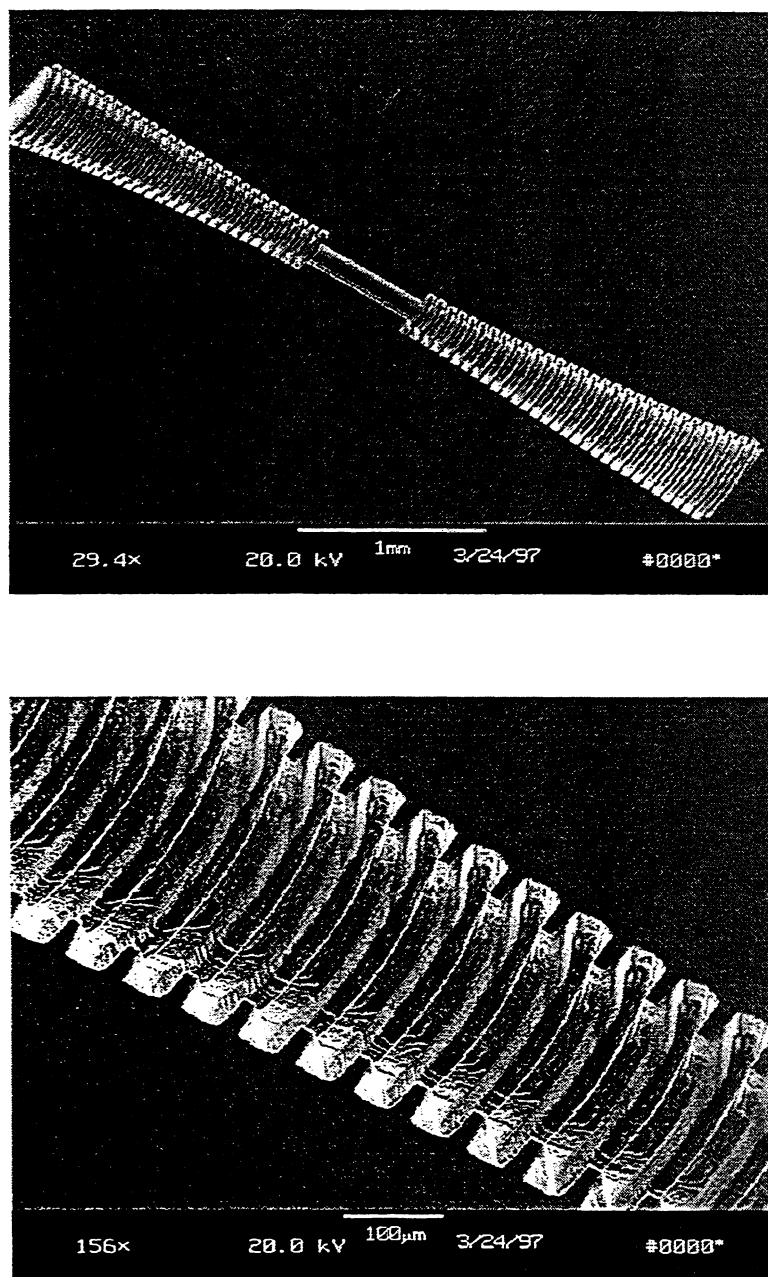
Figure 5: (a) SEM micrograph of replicated version of 2 THz waveguide structure. The original structure was etched using 3 Watts of laser power focused into a 4 μm spot in 200 Torr of chlorine gas. The laser beam was scanned at 4 cm/s and incrementally moved 2 micrometers between line scans removing 0.65 μm shavings per pass of the laser over the surface. (b) SEM close-up of ridges.

2.2 Device Replication

Although the process can be used to produce prototypes relatively quickly, to produce large format arrays, it becomes more practical to replicate the etched devices. We are currently working on a polymer based replication process [11] to produce high performance, low-cost, focal plane arrays at THz frequencies. This molding process has shown extremely high fidelity in reproducing features down to sub-micrometer detail. A negative of the silicon etched master is first made by casting polydimethylsiloxane (PDMS) over the etched surface which has been first fluorinated with tridecafluoroctaltrichlorosilane (TDTS). Due to the high elastomeric constant and low interfacial free energy between PDMS and the surface, it can be readily pulled apart from the silicon master. A low-viscosity polymer precursor, such as uv-curable epoxy, polyurethane, or polymethylmethacrylate is then flowed over the elastomer negative, filling the structure through capillary action. After curing, the elastomer is pulled from the epoxy replica for further reuse. A portion of a replicated version in five minute uv-cured epoxy of a 2.0 THz waveguide structure is shown in Figure 6 showing the excellent fidelity of the process. After the structures are replicated in epoxy, 0.3 μm of gold are sputtered onto the waveguide surface. The structures are then mated using uv-cureable epoxy in a double sided aligner we have implemented. Cross-hairs etched off to the side of the waveguide on the silicon master and masked during the gold sputtering are used as guides in the mating procedure. A summary of the replication and coating process is shown in Table 1.

3 Beam Pattern of a 2 THz Laser Micromachined Feedhorn

Using the process described above, two 2 THz corrugated feedhorns were fabricated in an end-to-end arrangement as shown in Figure 5a. The feedhorn design follows that of [12] and has 30 corrugations. The two horns are connected by a short (0.164 mm) section of circular waveguide. Once the two halves of the horn blocks have been aligned and mated, they are clamped into a test fixture (Figure 7). The beam of one feedhorn looks through a far-infrared, low-pass filter (0.8 mm thick crystalline quartz with garnet powder and a black
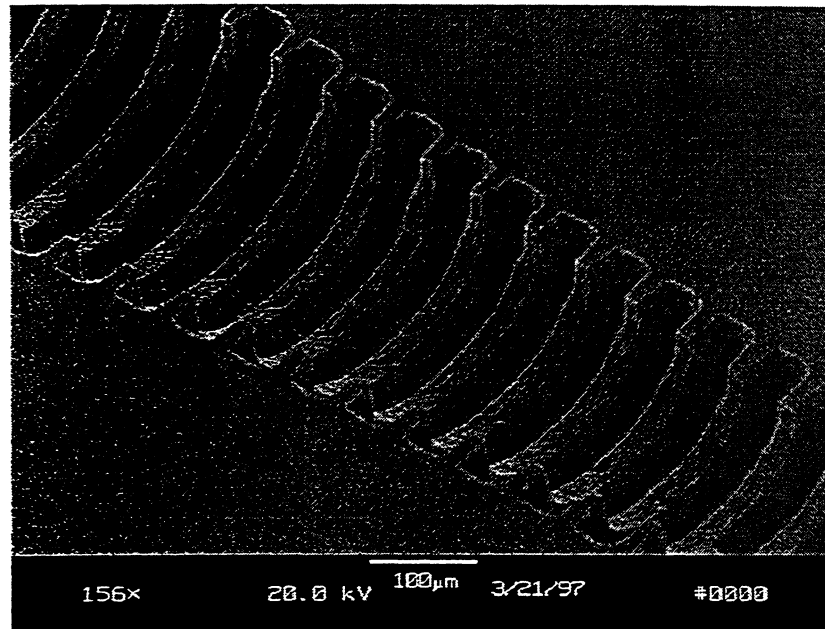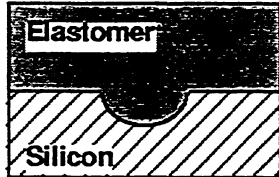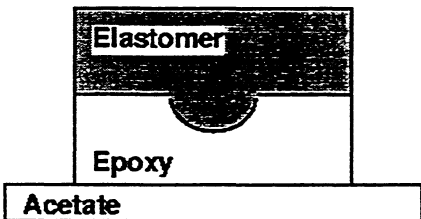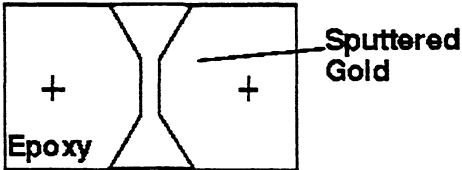
Figure 6: SEM micrograph of replicated version of 2 THz waveguide.

polyethylene layer) and polyethelene vacuum window into an anechoic chamber. It is this feedhorn on which the beam pattern measurement is performed. An additional ($\sim 25\mu m$) layer of black polyethylene was placed across the vacuum window to further reduce the possibility of near/mid infrared light leaks. The second feedhorn looks down into a reflective cavity containing a doped silicon bolometer [13] designed to operate at 4 K. Together the low-pass filter and feedhorns limit the frequency response of the bolometer to between ~ 1.4 and 2.4 THz. The voltage output of the bolometer is proportional to the power intercepted by the input feedhorn over this frequency range. The downward looking cryostat containing the detector assembly is mounted on top of an air tight anechoic chamber as shown in Figure 8. The humidity in the chamber can be lowered by filling it with dry nitrogen gas and/or with a tray of dessicant. The chamber contains a large (42" travel), computer-controlled, X-Y stage. A calibrated, upward looking, black-body source is mounted on the stage and serves as the signal source for beam pattern measurements. For the measurements described here, the temperature of the blackbody source was set to 950 K. The blackbody aperture is

Table 1: Replication and Gold Sputtering Process

1. LASER ETCH WAVEGUIDE	
	Silicon
2. PRIME SUBSTRATE WITH RELEASE AGENT AND CREATE ELASTOMER MASTER FROM PDMS (NEGATIVE TONE)	Elastomer / Silicon
3. REPLICATE ELASTOMER IN UV-CURED EPOXY ON ACETATE SUBSTRATE	Elastomer / Epoxy / Acetate
4. PEEL OFF ELASTOMER AND ACETATE AND SPUTTER GOLD ON EPOXY REPLICA	Sputtered Gold / Epoxy

chopped at 20 Hz. Beam pattern measurements are made by scanning the blackbody under the test dewar and synchronously detecting the bolometer output using a lock-in amplifier. The control computer records the position of the black body source along with the corresponding lock-in amplifier output. The distance between the black body source and feedhorn (234 mm) provides an angular resolution of $\sim 1.47°$.

Figure 9 shows cross-scans of the 2 THz feedhorn. The plots indicate the feedhorn's beam is nearly Gaussian with no measurable sidelobes to the noise floor of the map (~ 11 dB). There is a small asymmetry in the beam patterns, probably the result of a slight misalignment between the two halves of the horn block. The FWHM of the beam profile is $\sim 20°$, close to the value of 19.3° derived from the horn's beamwaist, $\omega_o = 0.33\,d$, where d is the diameter of the feedhorn aperture ~ 0.506 mm.
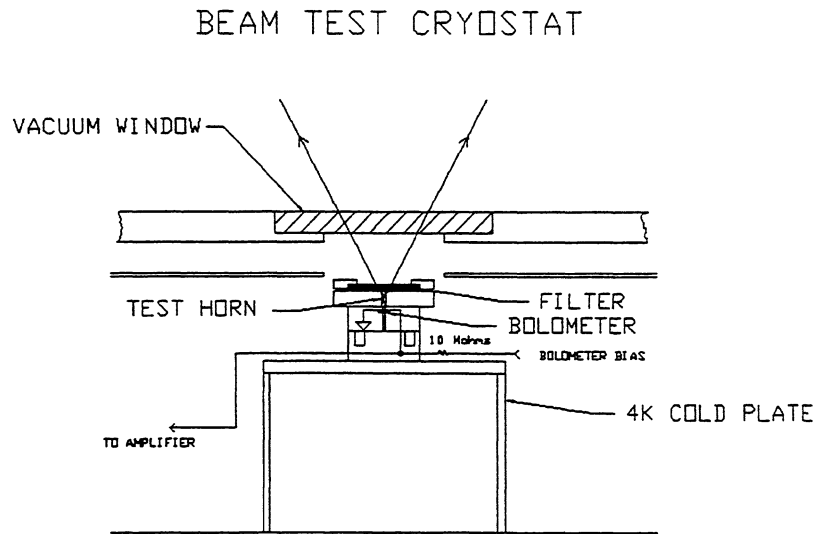
Figure 7: Cross section of feedhorn test fixture mounted in the cryostat. The beam of one feedhorn looks through a far-infrared, low-pass filter (0.8 mm thick crystalline quartz with garnet powder with a black polyethylene layer) and polyethelene vacuum window into an anechoic chamber. The second feedhorn looks down into a reflective cavity containing a doped silicon bolometer [13] designed to operate at 4 K.

4 Applications

4.1 Mixer Arrays

With this new micromachining technology it is now possible to consider the construction of large format arrays of high-performance THz waveguide receivers. Figures 10, 11a, 11b, and 11c illustrate how a 2 THz array of hot-electron bolometer mixers could be constructed using this technology.

Figure 10 is an assembly diagram of the mixer array. The design uses an array of corrugated feedhorns, each with a reduced-height waveguide transition (Fig. 11a). The
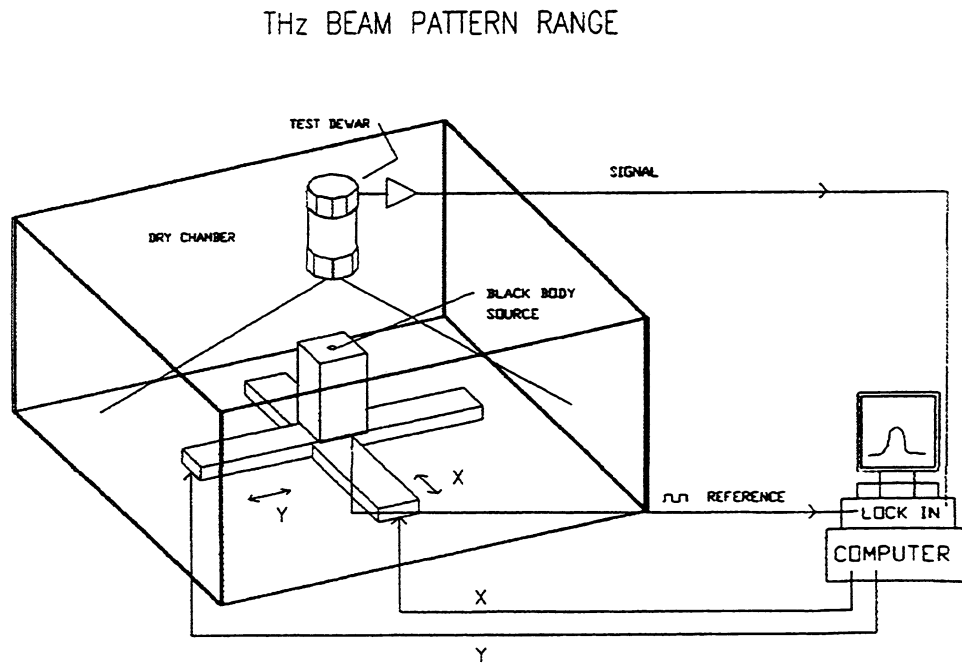
THz BEAM PATTERN RANGE

Figure 8: THz Beam Pattern Range. The chamber contains a large (42″ × 42″ travel), computer-controlled, X-Y stage. A calibrated, upward looking, black-body source is mounted on the stage and serves as the signal source for beam pattern measurements.

reduced-height waveguide should provide an excellent match to the real part of the bolometer impedance, permitting the use of only a single, fixed backshort.

At high frequencies (≥ 650 GHz) it becomes nearly impossible to manually mount detectors across small waveguide structures. In order to avoid this problem, mixing devices for the array are fabricated on ~1 μm thick silicon nitride membranes. To date, this approach has been successful with SIS junctions up to frequencies of ~850 GHz. Here, the bolometers are fabricated on membranes which span an aperture with the dimensions of the reduced height waveguide used in the 'horn block'. These apertures are formed by etching a pyramidal hole from the backside of the silicon wafer supporting the membrane (see Fig. 11b). As with the horn block, all exposed surfaces of silicon are gold plated to provide conduction. The bolometers are placed in the center of the waveguide. Low pass filtering is provided by a
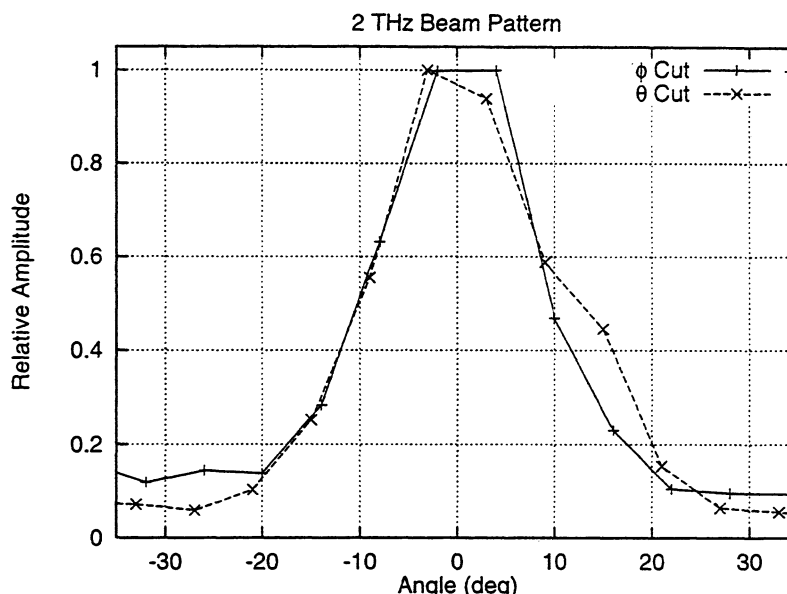
Figure 9: Beam cross scans of the micromachined 2 THz feedhorn. The θ and ϕ cuts are othogonal to each other.

microstrip circuit (see Fig 11c). Each IF output of the array is wire bonded to a microstrip matching network located just outside the periphery of the Bolometer Array Block. Bolometer bias is provided through the matching network.

The fixed backshort is a pyramidal structure designed to fit the cavity behind the membrane. The backshorts can be readily made by wet-etching silicon through an SiO mask evaporated on the wafer [2]. Once etched, the backshort wafer is gold plated.

4.2 Other Applications

With laser micromachining it now becomes possible to incorporate reactive posts and irises in submillimeter waveguide designs. These structures would be particular useful in providing a low-loss alternative to the end-loaded and radial stubs often used to tune out the capacitance of SIS junctions in waveguide mixer mounts. Below the gap frequency of niobium (~ 690 GHz), where such stubs are less lossy, the addition of a properly chosen post or iris can increase the instantaneous bandwidth of the mixer significantly over what would be achieved with the tuning stub alone.

Corrugated feedhorn with
waveguide transition to
reduced height rectangular
waveguide

Wire bonding pads

Niobium microbridge bolometer
on 1 um thick silicon nitride
membranes

IF output transmission line

Pyramidal Backshorts

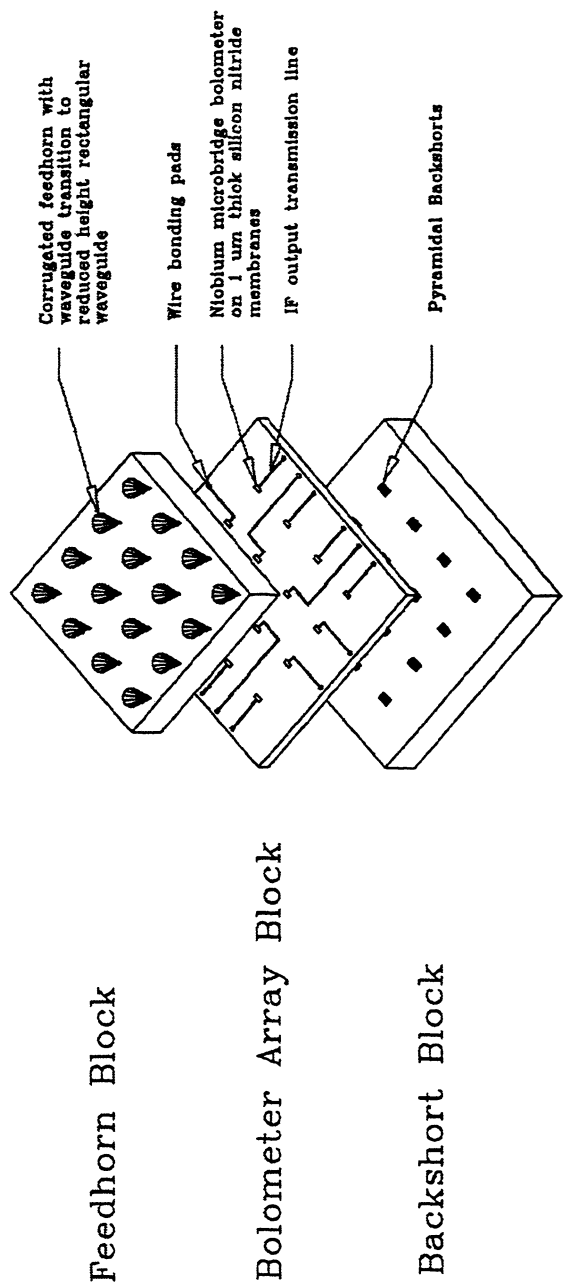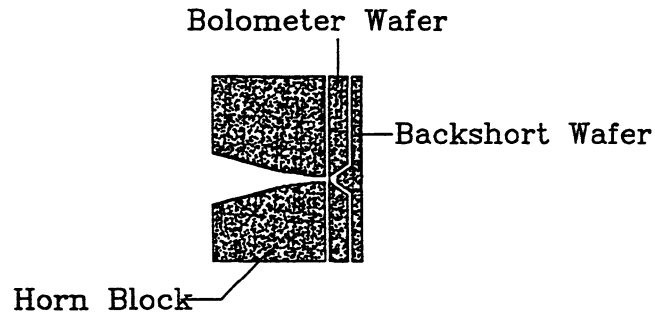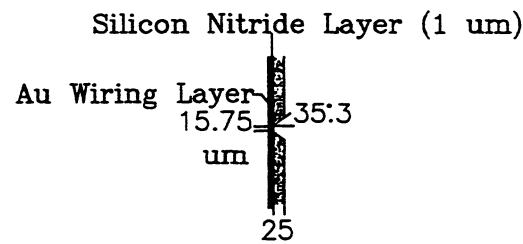Feedhorn Block

Bolometer Array Block

Backshort Block

Figure 10: Silicon micromachined array mixer assembly diagram. The array mixer consists of three blocks: a feedhorn block, a bolometer array block on which HEBs are fabricated across silicon nitride windows, and a backshort block. The horn block is laser micromachined. The bolometer array block and the backshort block are micromachined out of silicon using wet etching techniques.
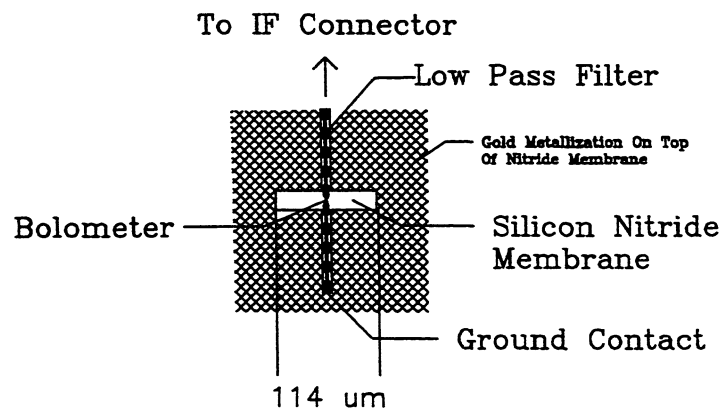
(a) Cross—section View of Mixer Assembly

Bolometer Wafer

—Backshort Wafer

Horn Block—

(b) Junction Wafer Block

Silicon Nitride Layer (1 um)

Au Wiring Layer
15.75 35:3
um

25

Side View

(c) Front View of Junction Wafer

To IF Connector

—Low Pass Filter

Gold Metallization On Top
Of Nitride Membrane

Bolometer —

— Silicon Nitride
Membrane

— Ground Contact

114 um

Front View

Figure 11: Detailed drawings of a typical mixer in the array.

The design and construction of solid state frequency multipliers is often more difficult to achieve than a single mixer [14]. The ability to micromachine reduced height waveguide with the option of including irises and posts, will allow the designer greater flexibility in the construction of high efficiency THz LO sources than have been available in the past.

Laser micromachining can also be used to make high performance submillimeter-wave phase gratings [15, 16]. These gratings can serve as quasi-optical LO power splitters for submillimeter array receivers.

The laser micromachining and replication process permits the construction of large numbers of high-efficiency feedhorns. Such horns could provide an alternative to Winston cones in large format bolometer arrays where single mode optics are desired.

5 Summary

1. We have introduced a new technology for the fabrication of waveguide devices which are difficult or impossible to manufacture using conventional techniques. We envision structures operating at 1 through 10 THz (feature sizes of 300-30 micrometers) can be fabricated with this technology.

2. With this technology it is now possible to construct large-format, waveguide imaging arrays at THz frequencies.

3. This technology can also be used in the construction of efficient LO sources and quasi-optical components at THz frequencies.

6 References

1 R. McGrath, C. K. Walker, M. Yap, and Y. Tai, IEEE Microwave and Guided Wave Letters, vol 3, 61, 1993.

2 G. Rebeiz, G. W. Regehr, G. Wade, D. B. Rutledge, R. L. Savage, L. Richard, N. C. Luhmann JR, Int. J. of IR ans MM Waves, vol 8, 1249, 1987.

3 D.J. Ehrlich, R.M. Osgood, Jr., and T.F. Deutsch, Appl. Phys. Lett., 38, 1018, 1981.

4 G.V. Treyz, R. Beach, and R.M. Osgood, Jr., J. Vac. Sci. Technol. B. 6, 37, 1988.

5 G.V. Treyz, R. Beach, and R.M. Osgood, Jr., Appl. Phys. Letters 50, 475, 1987.

6 T.M. Bloomstein and D.J. Ehrlich, in Technical Digest of Transducers (IEEE, New York, 1992), pp. 507-511, 1991.

7 T.M. Bloomstein and D.J. Ehrlich, Appl. Phys. Lett. 61, 708, 1992.

8 Y.S. Liu, "Sources, optics, and laser microfabrication systems for direct writing and projection lithography" in Laser Microfabrication, edited by D.J. Ehrlich and J.Y. Tsao (Academic Press, San Diego, ch. 1., 1989.

9 See M3 Scanner/Driver User's Manual, Rev. A (General Scanning, Inc. Watertown, MA, 1992).

10 T.M. Bloomstein, Sc.D. Thesis, Massachusetts Institute of Technology, 1996.

11 E. Kim, Y. Xia, and G.M. Whitesides, Nature 376, 581, 1985.

12 B. M. Thomas, IEEE Trans. Antennas and Propagation, 26, 267, 1978

13 Infrared Laboratories Inc., 1808 E 17th St., Tucson, Az.

14 N. Erickson, 1997, this volume.

15 G. F. Delgado and Bengtsson, 1194, Microwave and Optical Technology Letters, vol. 7, No. 18, pp. 831-834.

16 T. Klein, G. A. Ediss, R. Güsten, C. Kasemann, 1997, this volume.